Femtosecond nonlinear coherence spectroscopy of carrier dynamics in porous silicon

Lap Van Dao[a] and Peter Hannaford
Centre for Atom Optics and Ultrafast Spectroscopy, Swinburne University of Technology, Melbourne, Australia 3122

(Received 16 May 2005; accepted 31 August 2005; published online 19 October 2005)

Multidimensional nonlinear coherence spectroscopy based on spectrally resolved femtosecond two-color three-pulse photon echo measurements are used to investigate carrier dynamics and energy structures in porous silicon samples, an indirect band-gap material. Short time scales for electron localization (~500 fs) and electron hopping (~3 ps) are observed which are dependent on the porosity of the samples. A spin-orbit splitting for the conduction band of 4–5 meV is deduced. The observed energy splittings of 18 and 22 meV for the 48% porosity sample and 21 and 28 meV for the 70% porosity sample are assigned to spin-orbit splitting for the valence band. © *2005 American Institute of Physics*. [DOI: 10.1063/1.2102070]

I. INTRODUCTION

The field of quantum structures such as quantum wells, quantum wires, and quantum dots has been a fascinating field of materials science for the past two decades. The efficient emission of light from porous siliconl (Si) (Ref. 1) and Si nanostructures[2,3] involving quantum confinement effects has led to current interest in porous Si because on one hand light-emitting nanostructures can be fabricated without expensive equipment such as lithographic or epitaxial equipment and on the other hand Si is the most technologically important material known to mankind. Light-emitting Si devices could result in the development of Si technology from microelectronics to optoelectronics. The light emission is possible in porous silicon (PS) because of quantum confinement effects. The quantum confinement in PS results in enlargement of the band gap and efficient emission in the visible wavelength range at room temperature.

The optical properties of micro-PS have been studied by different techniques such as photoluminescence[4] in various types of PS, but the origin of the light emission is still under debate. Macro- and meso-PSs have also received much attention as good candidates for making microcavities and photonic crystals[5,6] or mirrors[7] with porous multilayers. However, since meso-PS consists of Si wires with diameters of 6–10 nm, the quantum confinement does not strongly modify their electronic states and quantum efficiency for light emission is rather low, making studies of the optical properties of meso-PS more difficult. The different size and shape of porous wires[8] will result in a broad distribution of confinement energies and the highly inhomogeneous structure of the material leads to difficulty in determining the energy states of PS. The existence of free charge carriers in porous silicon is a complex problem which involves questions such as carrier localization, compensation, and the binding energy of charge carriers in nanocrystals.

Conventional time-resolved techniques such as transient absorption[9] are not able to study an indirect gap material such as silicon. Time-resolved photoluminescence,[10] (PL) can be used to study long carrier lifetimes in PS,[1] but the time resolution is not very high for a sample with a low PL intensity signal because a wide time window has to be used, and therefore fast processes such as the capture and localization of the carriers cannot be studied in detail. In femtosecond multiple-pulse coherence spectroscopy[11] the signals are generated when the multiple pulses interact with the same states or coupled states, which allows separation of the homogeneous and inhomogeneous broadenings of the system and studies of the dynamics of the excited carriers on a very short time scale.[11–13] Thus this technique can be useful for investigating such indirect band-gap systems.

In this paper we report the use of spectrally resolved femtosecond two-color three-pulse photon echoes as a potentially powerful multidimensional technique for studying the optical properties and carrier dynamics of mesoporous silicon, which is an example of an indirect band-gap system. Control of two independent time delays, between the first and second pulses t_{12} and between the second and third pulses t_{23}, reveals the dynamics of the coherence and population ensembles, respectively. Furthermore, the wavelengths of the pump and probe pulses can be independently selected to drive particular quantum pathways and to study the dynamics of the electron or hole systems. With this technique more than three degrees of freedom can be independently controlled to provide detailed information about the energy structures and dynamics of the charge systems.

II. SPECTRALLY RESOLVED TWO-COLOR THREE-PULSE NONLINEAR SPECTROSCOPY

The spectrally resolved femtosecond two-color three-pulse photon echo measurements are carried out using three sequential femtosecond pulses (pulse duration <100 fs). The two pump pulses have wave vectors $\mathbf{k}_1$ and $\mathbf{k}_2$ and the same wavelength ($\lambda_1=\lambda_2$), and the probe pulse has wave vector $\mathbf{k}_3$ and a wavelength (λ_3) which can be shorter or longer than the pump pulse. The first pulse excites the porous silicon wires to generate electrons and holes in the band or in trap

[a]Electronic mail: dvlap@groupwise.swin.edu.au

levels with certain phase information. After a time t_{12} the second pulse interacts with the excited electrons and holes, and the phase information of the electrons and holes is stored in the population distribution of the electrons and holes, which depends on the position of the carriers in the energy levels. This phase and population distribution in frequency space gives rise to a frequency-modulated transmission spectrum of the sample. The frequency of this modulation is dependent on the time separation (t_{12}) of pulses $\mathbf{k}_1$ and $\mathbf{k}_2$, which is called the coherence time. The third pulse interacts with the population distribution at time t_{23}, putting the system in a superposition again, and a nonlinear signal is generated in the phase matching directions $\mathbf{k}_4=\mathbf{k}_3+\mathbf{k}_2-\mathbf{k}_1$ or $\mathbf{k}_5=\mathbf{k}_3-\mathbf{k}_2+\mathbf{k}_1$. When the first and third interactions create optical coherences having the same phase, a free induction decay signal is generated which carries information about the dephasing of the excited carriers. When the phase of the optical coherence created by the first and third interactions is opposite and the system has rephasing properties, a photon echo signal is generated at positive delay times near t_{12} after the third pulse interaction.[13]

For low laser intensities the nonlinear polarization is given by the third-order term $P^{(3)}$. The induced nonlinear polarization generates a signal electric field $E_S(t)$, which for low optical density and perfect phase matching is directly proportional to the nonlinear polarization. For interaction with three temporally separated optical pulses, having electric fields E_1, E_2, and E_3 and frequencies ω_1, ω_2, and ω_3, the third-order nonlinear polarization $P^{(3)}(t,t_{12},t_{23})$ depends on the time delays between the laser pulses.[13] Detailed information about the temporal evolution of the nonlinear polarization can be obtained by recording the spectrum of the nonlinear signal using a spectrometer.[11] The frequency-domain nonlinear polarization is determined by Fourier transformation of the time-domain nonlinear polarization with respect to t,

$$P^{(3)}(\omega,t_{12},t_{23})=\int_{-\infty}^{\infty}P^{(3)}(t,t_{12},t_{23})\exp(i\omega t)dt. \tag{1}$$

For a multilevel system the polarization results from a summation (approximately)[11] of the nonlinear polarization over n two-level systems,

$$\tilde{P}^{(3)}(\omega,t_{12},t_{23})=\sum\tilde{P}_n^{(3)}(\omega,t_{12},t_{23}). \tag{2}$$

The spectrally resolved photon echo (SRPE) signal intensity is then

$$S_{\mathrm{SRPE}}(\lambda_D,t_{12},t_{23})\propto|E_S(\omega,t_{12},t_{23})|^2\propto|\tilde{P}^{(3)}(\lambda_D,t_{12},t_{23})|^2, \tag{3}$$

where λ_D is the detection wavelength.

To simplify our understanding of the linear and nonlinear optical responses of a system we can describe the induced polarization, which decays with dephasing time T_2, in frequency space for a homogeneously broadened system as a Lorentzian function,

$$P(\omega)\sim f\Gamma/[(\omega-\omega_0)^2+\Gamma^2/4], \tag{4}$$

where f is the oscillator strength, $\Gamma=1/T_2$ is the linewidth, and ω_0 is the center frequency. Any optical system will produce a nonlinear response if one or more such parameters (f,Γ,ω_0) are changed by the interaction with the laser pulses.[14] For an inhomogeneously broadened system the induced polarization can be taken as the sum of several Lorentzians with different center frequencies.

When the first and second pulses temporally overlap (or partially overlap) in the sample, the pulses interfere to create a periodic standing-wave pattern, which can induce a *population grating* by absorption in the sample. In the present two-color three-pulse experiments in which $\omega_1=\omega_2\neq\omega_3$ the probe pulse can be diffracted by the population grating in the phase-matching direction $\mathbf{k}_4=-\mathbf{k}_1+\mathbf{k}_2+\mathbf{k}_3$ with frequency $\omega_4=\omega_3$. In this case the spectrum of the population grating signal is determined by the spectral profile of the probe pulse $I_{\mathrm{probe}}(\lambda_D)$. The *total* nonlinear signal spectrum, including the contribution of the population grating, can then be written as

$$S_D(\lambda_D,t_{12},t_{23})=S_{\mathrm{SRPE}}(\lambda_D,t_{12},t_{23})+\eta(\lambda_D,t_{12},t_{23})I_{\mathrm{probe}}(\lambda_D), \tag{5}$$

where $\eta(\lambda_D,t_{12},t_{23})$ is the efficiency of the (transient) population grating, which is proportional to $[\exp(-t_{23}/\tau_{\mathrm{life}})-\exp(-t_{23}/\tau_{\mathrm{rise}})]$, and τ_{life} and τ_{rise} are the lifetime and buildup time of the population grating, respectively.

III. EXPERIMENTS

The ultrafast laser pulses are generated by two independently tunable optical parametric amplifiers (OPA) in the sum-frequency generation option (100 fs, 1–30 μJ) pumped by a 1 mJ amplified pulse (80 fs, 800 nm, 1 kHz). The wavelength of the laser pulses is in the visible region (550–650 nm) where the so-called "*S*-band" luminescence of porous silicon has received the most attention.[1] The output of one OPA is split into two beams, which act as the pump pulses ($\mathbf{k}_1$ and $\mathbf{k}_2$) and the output of the second OPA acts as the probe pulse ($\mathbf{k}_3$). Three beams with time delays t_{12} (between pulses $\mathbf{k}_1$ and $\mathbf{k}_2$) and delay t_{23} (between pulses $\mathbf{k}_2$ and $\mathbf{k}_3$) are aligned in a triangular configuration and focused by a 20 cm focal length lens into a 300-μm-diameter spot where the sample is placed.[11] The energy density of each pulse is about 1 mJ/cm^2 at the sample spot. The signal is generated from the sample in the phase-matching directions $\mathbf{k}_4=-\mathbf{k}_1+\mathbf{k}_2+\mathbf{k}_3$ and $\mathbf{k}_5=-\mathbf{k}_2+\mathbf{k}_1+\mathbf{k}_3$ which are detected simultaneously by a spectrometer equipped with double charge-coupled device (CCD) arrays having a spectral resolution <1 nm. The spectra are measured over a range of different fixed coherence times t_{12} or population times t_{23} by scanning the other delay time t_{23} or t_{12}, respectively. For studies of the influence of porosity on the carrier dynamics two meso-PS samples with porosities 48% and 70% are used. The preparation of the samples has been described elsewhere.[5,7] For better control of the porosity and the thickness of the porous layer a p-doped Si wafer has been used where the existence of free holes is expected.[7] The difference of the wavelength of the pump and probe pulses is ±15 nm which is larger than

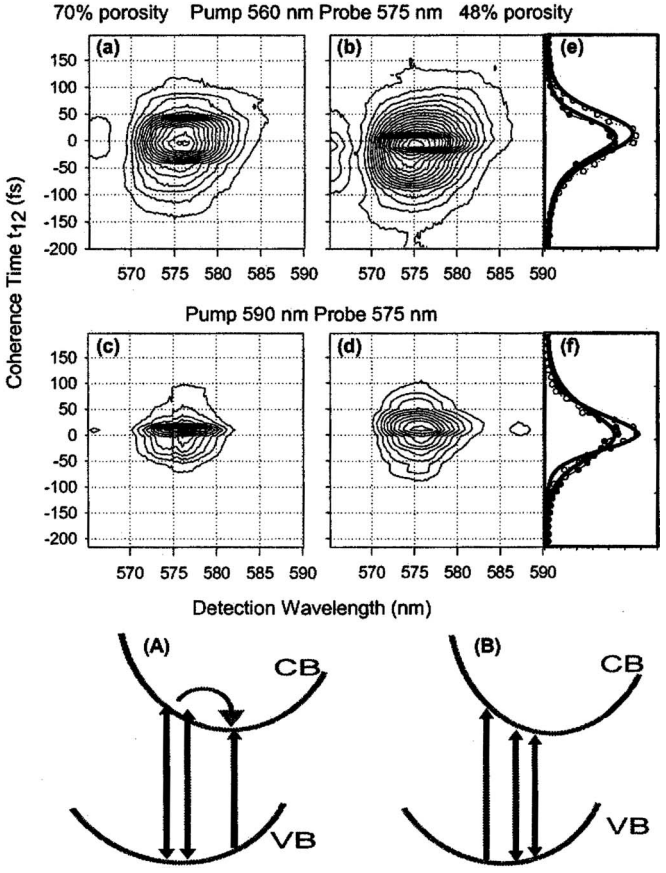

FIG. 1. Spectra of the nonlinear signal in the $\mathbf{k}_4=\mathbf{k}_3+\mathbf{k}_2-\mathbf{k}_1$ direction vs coherence time t_{12} with fixed $t_{23}=0$ and $\lambda_3=575$ nm for (a) a sample with 70% porosity and $\lambda_1=\lambda_2=560$ nm, (b) a sample with 48% porosity and $\lambda_1=\lambda_2=560$ nm, (c) a sample with 70% porosity and $\lambda_1=\lambda_2=590$ nm, and (d) a sample with 48% porosity and $\lambda_1=\lambda_2=590$ nm. The pulse interaction is illustrated in (A) $\lambda_1=\lambda_2<\lambda_3$ and (B) $\lambda_1=\lambda_2>\lambda_3$; CB: conduction band; VB: valence band. The signal intensity at 575 nm with a spectral window of 1 nm is displayed in (e) for the case in Figs. 1(a) (closed dots) and 1(b) (open dots), and (f) for the case in Figs. 1(c) (close dots) and 1(d) (open dots).

the full width at half maximum of the laser pulses ($\sim$10 nm). When the wavelength of the pump pulse is shorter than that of the probe pulse the dynamics of the electrons can be enhanced.

IV. RESULTS AND DISCUSSION

Figure 1 shows spectra of the signal detected in the $\mathbf{k}_4$ direction with $t_{23}=0$ versus coherence time t_{12}. The wavelength of the probe pulse is 575 nm and the wavelengths of the pump pulse are 560 nm [Figs. 1(a) and 1(b)] and 590 nm [Figs. 1(c) and 1(d)]. The intensity profile of the signal at 575 nm with a spectral window 1 nm is shown in Figs. 1(e) and 1(f), respectively. A similar spectrum evolution with slight variations for negative times $t_{12}<0$ is obtained for a range of fixed t_{23} from -120 to 120 fs. For times $t_{12}<0$ the pulse sequence is $\mathbf{k}_1,\mathbf{k}_2,\mathbf{k}_3$ and the observation of a photon echo is expected while for times $t_{12}>0$ the pulse sequence is $\mathbf{k}_2,\mathbf{k}_1,\mathbf{k}_3$ and the signal is generated by free induction decay (FID).[11,13] When the energy and population relaxations are much longer than the dephasing time the FID signal reflects only the dephasing of the optical transition and not the temporal evolution related to energy or population relaxation processes in the sample. The photon echo signal should be more sensitive to the redistribution of the excited carriers because the generation of the signal involves rephrasing processes.

When the laser pulses interact with an inhomogeneously broadened system the shape of the observed spectrum is time dependent because the result of the interaction of the laser pulses is different for each homogeneous mode. When the wavelength of the pump pulse is shorter than that of the probe pulse [Figs. 1(a) and 1(b)] a broadening of the signal spectrum on the long wavelength side and an asymmetric signal profile versus time delay for certain detected wavelengths is observed [Fig. 1(e)]. The decay time of the signal versus negative t_{12} at 575 nm is 43 fs (for the 70% porosity sample) and 45 fs (for the 48% porosity sample) which are related to the effective dephasing time T_2 given by $1/T_2=1/T_1+1/T_2^*$, where T_1 is the carrier lifetime and T_2^* is the "pure" dephasing time. Similar results are obtained when the probe wavelength is tuned to 590 nm and the pump wavelength to 575 nm. A photon echo peak shift, which is defined as the shift of the photon echo maximum at $t_{12}=0$ (Ref. 15) and which can be used to study the dynamics of the inhomogeneous broadening of the system,[15] is not observed in our measurements.

A broadening of the photon echo spectrum only for the case of a longer probe wavelength [Figs. 1(a) and 1(b)] is possible when free holes exist in the system and the excited electron ensemble moves toward the band edge, as illustrated in the Fig. 1(a). This motion is not possible when the pump wavelength is longer than that of the probe [Fig. 1(b)]. The existence of free holes in meso-PS is a result of the use of heavily doped p-type Si in which doping impurities are not removed during the electrochemical formation process.[16]

Figure 2 shows a photon echo spectrum versus delay time t_{23} with fixed $t_{12}=0$ during the first 1 ps. The time evolution of the signal intensity at 575 nm with a spectral window of 2 nm is shown in Figs. 2(a) and 2(b). A similar spectrum is observed for fixed $t_{12}=\pm 40$ fs but the intensity is weak. Clear oscillations in the signal intensity profile can be seen in Figs. 2(a) and 2(b). When the laser pulses span or partially span two (or more) transitions with frequencies ω_i and ω_j, different quantum pathways can be involved during the interaction of the system with the laser pulses, which can interfere, and the time-integrated signal versus delay time t_{12} or t_{23} exhibits oscillations (or quantum beats) at the difference frequency $\Delta\omega=|\omega_i-\omega_j|$. In a spectrally resolved measurement, the photon echo signal is detected for those transitions with frequencies equal to the detection frequency of the spectrometer ω_D. For the case of coupled oscillators there can be multiple quantum pathways having different initial (ω_j) and final frequencies (ω_i) which lead to the same detection frequency ω_D.[11,14] The relative phase difference between the quantum pathways gives rise to quantum beats at frequency $\Delta\omega$ in the photon echo signal as a function of t_{12} and t_{23}. The beating is present for the duration of the population time.[14,15,17]

Fourier spectra of the time evolution signal (up to 3 ps), e.g., in the inset of Fig. 2(b), can be used to deduce the

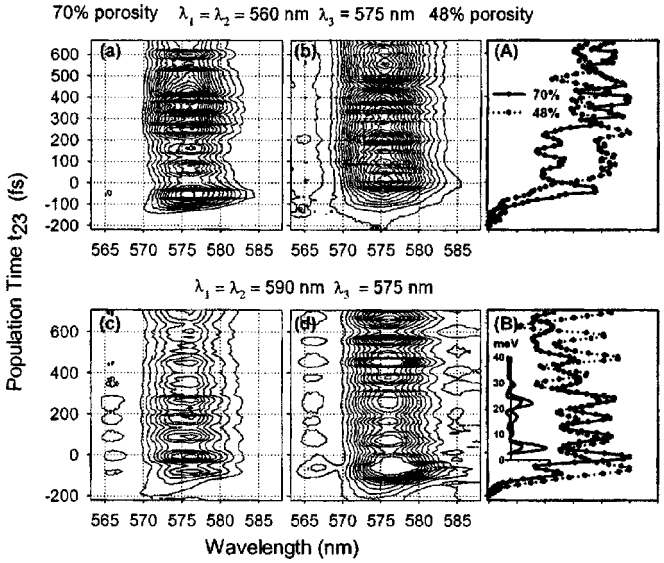

FIG. 2. Spectra of the nonlinear signal in the $\mathbf{k}_4=\mathbf{k}_3+\mathbf{k}_2-\mathbf{k}_1$ direction vs population time t_{23} with fixed $t_{12}=0$ and $\lambda_3=575$ nm for (a) a sample with 70% porosity and $\lambda_1=\lambda_2=560$ nm, (b) a sample with 48% porosity and $\lambda_1=\lambda_2=560$ nm, (c) a sample with 70% porosity and $\lambda_1=\lambda_2=590$ nm, and (d) a sample with 48% porosity and $\lambda_1=\lambda_2=590$ nm. The signal intensity at 575 nm with a spectral window of 2 nm is displayed in (A) for the case in Figs. 2(a) and 2(b), and (B) for the case in Figs. 2(c) and 2(d). The inset in Fig. 2(b) shows the Fourier spectra for the two samples taken from a data set for the case $\lambda_1=\lambda_2=590$ nm and $\lambda_3=575$ nm.

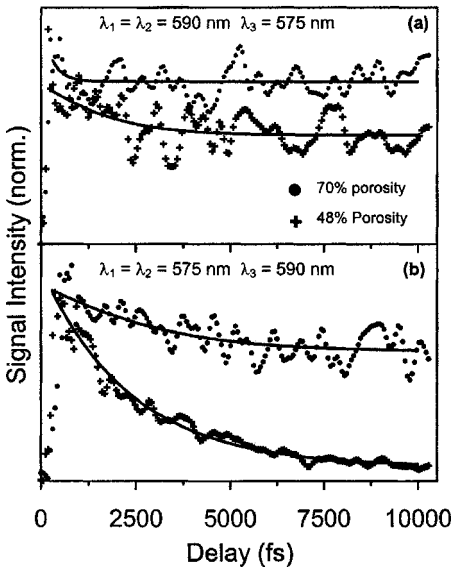

FIG. 3. Time-integrated signal intensity vs population time t_{23} with $t_{12}=0$ for two samples: (a) $\lambda_1=\lambda_2=590$ nm and $\lambda_3=575$ nm and (b) $\lambda_1=\lambda_2=575$ nm and $\lambda_3=590$ nm. The symbols represent the experimental data and the solid lines show the fits with a two-exponential decay function.

energy splitting of the coupled transitions. For all wavelength combinations and samples an energy splitting of 4–5 meV is observed which is close to the singlet-triplet splitting [6 meV (Ref. 18)] of crystalline Si or the spin-orbit splitting for the conduction band of PS quantum wires [3–7 meV (Ref. 8)]. Splittings of 18 and 22 meV are deduced for the sample with 48% porosity and 21 and 28 meV for the sample with 70% porosity. These splittings are related to the spin-orbit splitting of the valence band, around 20–35 meV.[8]

When the pump wavelength is shorter than the probe wavelength the rise time (time for signal reach its maximum) is longer (by up to 500 fs) for the sample with high porosity (70%), as seen in Figs. 2(a) and 2(a) for the case of a pump wavelength at 560 nm and probe wavelength at 575 nm. Similar results are obtained when a pump at 575 nm and probe at 590 nm are used. The rise time represents the time for localization of the excited electrons in the conduction band [Fig. 1(a)].

For long scans of the population time (up to 10 ps) a short decay time (~3 ps) and a very long decay time (>100 ps) are observed (Fig. 3). A two-exponential function has been used for fitting the decay times. When the probe wavelength is shorter than that of the pump pulse [Fig. 3(a)] the short decay component (~3 ps) is clearly observable for the low porosity sample and very small for the high porosity sample. The magnitude of the short decay component is much higher when the pump wavelength is shorter than the probe wavelength [Fig. 3(b)]. Due to the existence of free holes in these samples the variation of the optical properties reflects the dynamics of the electrons and the decay of the signal intensity indicates hopping of the electrons among the localized states. In the low porosity sample the time scale for electron hopping is shorter (probability is higher) because the number of surface states, where the carrier is localized,[19] is smaller than that for the high porosity sample. The observed signal versus population time provides the following picture for the excited carrier dynamics. In the first picosecond after excitation the photon-created carriers (mostly electrons) are trapped in localized states. The free holes excited in the meso-PS are trapped in surface states.[19] The electrons hop among the localized states and finally recombine nonradiatively with the holes. In contrast to micro-PS where the carrier hopping is absent[20] the hopping of excited electrons in meso-PS takes place on a rather short time scale (~3 ps) leading to very weak luminescence.

V. CONCLUSIONS

Spectrally resolved two-color three-pulse photon echo spectroscopy provides a potentially powerful multidimensional technique for studying the carrier dynamics of an indirect band-gap material such as silicon on a femtosecond time scale. The large number of available degrees of freedom in time delay scans and wavelengths of the laser pulses allows one to separate and extract certain specific types of spectroscopic information in complex systems. The use of different colors for the pump and probe pulses allows separation of the dynamics of the electrons and holes. The time (and spectral) evolution of the photon echo signal also allows the resolution of different quantum beat frequencies corresponding to different selected energy splittings.

ACKNOWLEDGMENTS

We thank Peter Reece and Michael Gal from the School of Physics, the University of New South Wales for supplying the porous silicon samples, and Mark Aizengendler and Alex Stanco from Lastek Laboratories for their contributions to

the spectrometer and Garry CCD detector. This project is supported by an Australian Research Council Discovery grant.

[1]A. G. Cillis, L. T. Canham, and P. D. J. Calcott, J. Appl. Phys. **82**, 909 (1997).
[2]L. V. Dao, X. Wen, M. T. T. Do, P. Hannaford, E. Cho, Y. Cho, and Y. Huang, J. Appl. Phys. **97**, 013501 (2005).
[3]Y. Kanemitsu and S. Okamoto, Phys. Rev. B **56**, R15561 (1997).
[4]C. Delerue, G. Allan, and M. Lannoo, Phys. Rev. B **48**, 11024 (1993).
[5]P. J. Reece, G. Lerondel, W. H. Zheng, and M. Gal, Appl. Phys. Lett. **81**, 4895 (2002).
[6]U. Grning, V. Lehmann, and C. M. Engelhardt, Appl. Phys. Lett. **66**, 3254 (1995).
[7]A. Bruyant, G. Lerondel, P. J. Reece, and M. Gal, Appl. Phys. Lett. **82**, 3227 (2003).
[8]G. D. Sanders and Y.-C. Chang, Phys. Rev. B **45**, 9202 (1992).
[9]W. Rudolph, J. Puls, F. Henneberger, and D. Lap, Phys. Status Solidi B **159**, 49 (1990).
[10]L. V. Dao, M. Gal, G. Li, and C. Jagadish, Appl. Phys. Lett. **71**, 1849 (1997).
[11]L. V. Dao, C. N. Lincoln, R. M. Lowe, and P. Hannaford, J. Chem. Phys. **120**, 8434 (2004).
[12]L. V. Dao, M. Lowe, and P. Hannaford, J. Phys. B **36**, 1719 (2003).
[13]S. Mukamel, *Principles of Nonlinear Optical Spectroscopy* (Oxford University Press, New York, 1995).
[14]L. V. Dao, R. M. Lowe, P. Hannaford, H. Makino, T. Takai, and T. Yao, Appl. Phys. Lett. **81**, 1806 (2002).
[15]W. Kaiser, in *Topics in Applied Physics* (Springer, Heidelberg, 1988), Vol. 60.
[16]M. Cho, J. Y. Yu, T. Joo, Y. Nagasawa, S. A. Passino, and G. R. Fleming, J. Phys. Chem. **100**, 11944 (1999), and references therein.
[17]J. M. Shacklette and S. T. Cundiff, Phys. Rev. B **66**, 045309 (2002).
[18]M. Rosenbauer, S. Finkbeiner, E. Bustarret, J. Weber, and M. Stutzmann, Phys. Rev. B **51**, 10539 (1995).
[19]V. Yu. Timoshenko, Th. Dittrich, V. Lysenko, M. G. Lisachenko, and F. Koch, Phys. Rev. B **64**, 085314 (2001).
[20]I. Mihalcescu, J. C. Vial, and R. Romestain, Phys. Rev. Lett. **80**, 3392 (1998).